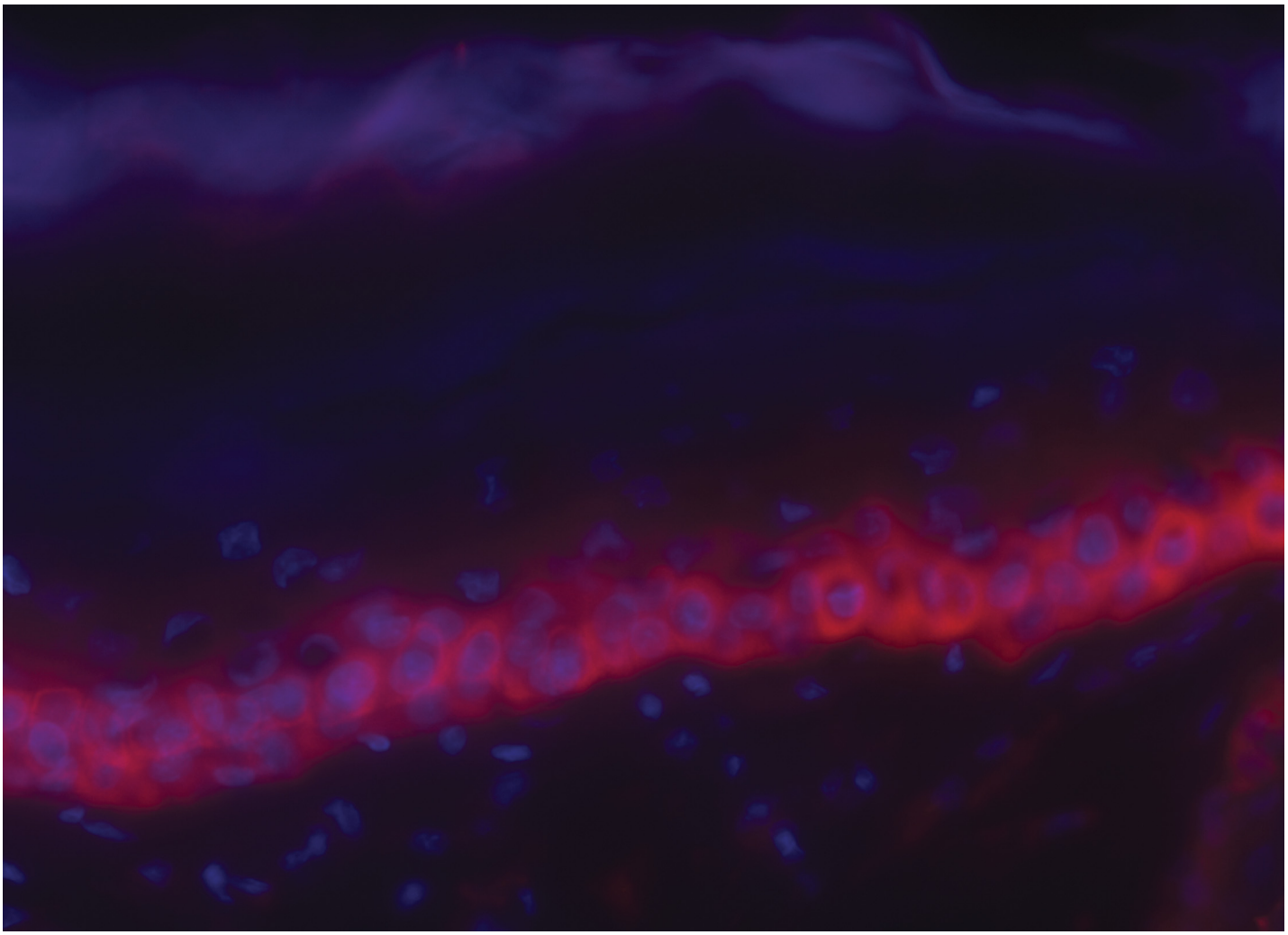

**Showcasing research from Professor Jonathan P. Singer's laboratory, School of Engineering, Rutgers University—New Brunswick, New Jersey, United States.**

Microneedle arrays coated with Middle East respiratory syndrome coronavirus DNA vaccine *via* electrospray deposition

Immunofluorescence of antigen (denoted in red) and skin cell nuclei (denoted in blue) in response to the dermal insertion of microneedle arrays coated with Middle East respiratory syndrome coronavirus DNA vaccine by efficient electrospray deposition.

Image reproduced by permission of Sarah Park (Rutgers University) from *Soft Matter*, 2025, **21**, 3207.

## As featured in:


See Jonathan P. Singer *et al.*, *Soft Matter*, 2025, **21**, 3207.

ROYAL SOCIETY OF CHEMISTRY

rsc.li/soft-matter-journal

Registered charity number: 207890

Soft Matter

PAPER

View Article Online
View Journal | View Issue



Cite this: *Soft Matter*, 2025, **21**, 3207

# Microneedle arrays coated with Middle East respiratory syndrome coronavirus DNA vaccine *via* electrospray deposition†

Sarah H. Park,[a] Isha R. Shah,[b] Nandita C. Jhumur,[b] Yaxin Mo,[b] Shalaka Tendolkar,[b] Emran O. Lallow,[c] Jerry W. Shan,[b] Jeffrey D. Zahn,[d] Joel N. Maslow,[c] Assimina A. Pelegri,[b] Hao Lin,[b] David I. Shreiber[d] and Jonathan P. Singer *[ab]

Microneedle arrays have been shown to be a minimally invasive method of transdermal drug delivery. However, methods to coat these arrays often require a reservoir of the active ingredient, leading to unused and wasted material. Electrospray deposition is a targeted coating method that offers a competitive alternative for coating microneedles. By architecting the charge landscape of the setup, this technology can achieve coating deposition efficiencies nearing 100%, with little to no material wasted during the coating process. A Middle East respiratory syndrome coronavirus DNA vaccine was used as the model material to assess deposition efficiency as well as the efficacy of fragile biological materials subjected to electrospray deposition. Trehalose and polystyrene-*block*-polyacrylic acid were used as excipients to encourage coating dispersion. These coatings were inserted into Sprague Dawley rats where the antigen was subsequently detected and located using immunohistochemistry. Both coatings, with and without excipients, showed that protein expression is achieved after the vaccine is subjected to electrospray, however, the presence of excipients qualitatively leads to a more disperse diffusion profile. Further, this work demonstrates the capability of electrospray deposition as a highly efficient method to coat microneedles for transdermal drug delivery.

Received 8th November 2024,
Accepted 11th March 2025

DOI: 10.1039/d4sm01322k

rsc.li/soft-matter-journal



## 1. Introduction

Due to their numerous advantages in resource usage and administration, microneedle arrays (MNAs) have become a promising alternative to the delivery of bioactives.[1–3] MNAs can provide a minimally invasive method for delivering therapeutics and vaccines to various layers of the skin. Because the needles are only a few hundred microns in length, they penetrate the epidermis, which is abundant in antigen-presenting cells (APCs), leading to potential dose-sparing in vaccine delivery applications.[4–6] By targeting a region of the body with a high perfusion of APCs, immune responses elicited within the skin have been found to be stronger than immune responses observed intramuscularly.[2,7,8] In addition to potential dose-sparing, the hundreds of microns-length MNAs significantly reduce pain experienced by patients when compared to intramuscular vaccinations with hypodermic needles and, thereby, may improve patient compliance.[9,10] More notably, a few recent studies suggest that coated MNAs could improve the immune response elicited from DNA-based vaccines where the advancement of DNA vaccines has been severely limited by low levels of protein expression.[11,12]

The use of electrospray deposition (ESD) to coat MNAs offers many additional benefits for drug and vaccine delivery. ESD is a spray processing technique that is commonly utilized in agriculture for spraying pesticides and fertilizers onto crops,[13,14] in automotive for fuel dispersion in engines[15] and paint application, in battery manufacturing for fabricating both the cathode and anode separators as well as the anodic material,[16,17] and in photovoltaics for fabricating thin films capable of light harvesting.[18,19] Recently, we have demonstrated that ESD can also be an efficient process for the deposition of bioactive materials on targets smaller than the spray plume, achieving coating deposition efficiencies nearing 100% on MNAs.[20] Other methods of coating MNAs (*e.g.*, dip coating or inkjet printing) can often lead to material waste as these methods require a reservoir of coating material, and thus unused material,

[a] *Department of Materials Science and Engineering, Rutgers University–New Brunswick, Piscataway, NJ 08854, USA. E-mail: jonathan.singer@rutgers.edu*
[b] *Department of Mechanical and Aerospace Engineering, Rutgers University–New Brunswick, Piscataway, NJ 08854, USA*
[c] *GeneOne Life Science, Seoul, Republic of Korea*
[d] *Department of Biomedical Engineering, Rutgers University–New Brunswick, Piscataway, NJ 08854, USA*

† Electronic supplementary information (ESI) available. See DOI: https://doi.org/10.1039/d4sm01322k

or result in coating undesired regions of the substrate. Drainage effects observed with dip coating often leads to the contamination of the array base as well as wasted material.[21] Inkjet printing requires meticulous solution formulation to achieve uniform coatings and to avoid clogging the nozzle for inkjet printing. Although this coating method can be highly accurate, it comes at the expense of requiring serial processing, leading to elongated process times.[3,22] Conversely, ESD is capable of minimizing wasted material by targeting a grounded substrate with charged droplets of material and could be a competitive alternative for thin film coating fabrication. As with other dry coating methods, the electrosprayed coating is a thermostable solid, which is promising for distributing vaccines and therapeutics to resource-scarce regions of the world without widespread cold storage chains.[1,23] One key consideration, however, is how the electrohydrodynamic forces that drive ESD affect the integrity of the payload, and while our previous study demonstrated that much of the DNA structure appears to be retained in efficient coatings, it remains to be shown whether these coatings can be effectively transfected.

In ESD, a high voltage is applied onto a flowing dilute solution, and the resulting electrostatic force induces shear stress at the meniscus of the liquid, forming it into a Taylor cone. From this process, charged droplets emerge due to instabilities caused by competing surface tension and Coulombic interactions. These charged droplets then move towards a grounded substrate for targeted coating.[24] An advantage of ESD is that the droplet diameter can be manipulated by the flow rate and the applied voltage to achieve droplet diameters on the micro- and nano-scale.[24,25] However, the shear stress induced at the Taylor cone has been found to cause irreversible damage to fragile materials, thus possibly lowering the efficacy of the therapeutic.[15,26] Marchetti *et al.* reported that DNA condensation in high ethanol-content solutions can protect plasmids from this effect.[26,27] As a result, our work incorporates a high concentration of ethanol to help reduce the shear stress observed by plasmid DNA in our spray solution. In addition to retaining the structural integrity of these fragile materials, the coating formulation is equally crucial for therapeutics delivery. The coating formulation can critically impact efficacy in multiple ways, including protection of the therapeutic payload, improving the mechanics of the coating to ensure integrity during microneedle insertion, and potential enhancement of the release and dissolution of the payload after insertion. To demonstrate the ease of formulation in ESD, trehalose and polystyrene-*block*-poly(acrylic acid) (PS-*b*-PAA) were used in this study as example excipients that (1) aid in stabilizing and dissolving plasmid DNA and (2) improve the coating mechanics, respectively.

In this study, we compare the effectiveness of ESD-coated MNAs in delivering vaccine with and without excipients. Plasmid green fluorescent protein (pEGFP-N1) was electrosprayed and used for *in vitro* transfection of human embryotic kidney (HEK293T) cells to compare the transfection of sprayed pEGFP-N1 to pEGFP-N1 stock solution. MNAs were then coated with a DNA plasmid vaccine for Middle East respiratory syndrome coronavirus (MERS-CoV) and were inserted into rats to express the encoded transgene. The antigens produced in response to the vaccine were then located using immunohistochemistry. Our work presents preliminary results for a potentially more cost-effective and efficient coating method for fabricating coated MNAs.

## 2. Methods

### 2.1. Materials

D-(+)-trehalose ≥99%, polystyrene-*block*-poly(acrylic acid) (30 000 : 2000), and anhydrous 200 proof pure ethanol were obtained from Sigma Aldrich. Propidium iodide solution in water (1 mg $mL^{-1}$), Invitrogen MERS Coronavirus spike protein RBD polyclonal antibody, Invitrogen Alexa Fluor™ 546 goat anti-rabbit secondary antibody, Cytiva HyClone HyPure water, Prolong™ diamond antifade mountant with DAPI, Promega FuGENE™ HD transfection reagent, normal goat serum, and aqua-hold pap pen were obtained from Fisher Scientific. MERS-CoV DNA vaccine suspending in distilled $H_2O$ water for injection (GLS-5300)[28] and pEGFP-N1 were obtained from GeneOne Life Science, Inc. HEK293T (CRL-1573) cells were obtained from ATCC.

### 2.2. Electrospray solution preparation

Solutions were prepared by mixing 100 μL of 2.5 mg $mL^{-1}$ GLS-5300 vaccine or 100 μL of 2.5 mg $mL^{-1}$ pEGFP-N1 with 400 μL of 200 proof ethanol. For solutions including trehalose and PS-*b*-PAA, 5 μL of 25 mg $mL^{-1}$ trehalose in DI water and 1 μL of 25 mg $mL^{-1}$ PS-*b*-PAA in ethanol were aliquoted into a 1.5 mL microcentrifuge tube. The tube was then placed into an oven at 70 °C to evaporate the solvent with the solids remaining. 100 μL of 2.5 mg $mL^{-1}$ plasmid DNA and 400 μL of 200 proof ethanol were then added to these tubes.

For solutions using propidium iodide (PI), GLS-5300 was intercalated with PI using Float-A-Lyzer G2 (3.5–5 kDa, 1 mL) dialysis device purchased from Repligen. 3 mg of GLS-5300 and 0.5 mg of PI was loaded into the tube. pp$H_2O$ was added to the tube for a final concentration 2.5 mg $mL^{-1}$ of GLS-5300. After 72 h, sample was collected to ensure PI not binded to GLS-5300 would be removed. 90 μL of 2.5 mg $mL^{-1}$ pure GLS-5300 was mixed with 10 μL of GLS-5300 intercalated with PI. 400 μL of 200 proof ethanol was then added after combining the plasmids together. This solution was then used for spraying experiments.

### 2.3. Electrospray setup

The setup used a syringe pump (Harvard Apparatus 11 Plus), a negative high power voltage power supply (Acopian Power Supply, N012HA5), two positive high voltage power supplies (Acopian Power Supply, P012HA5), a blunt stainless steel needle (SAI Infusion, 20-gauge, 0.5″), a steel guard ring (4 cm outer diameter, 2 cm inner diameter), 2 mm long stainless steel microneedles in a 4 × 4 array, and a humidity and temperature controlled environmental chamber (Electro-Tech Systems, Inc.). The chamber had a controlled humidity ranging from 20–21% RH, and the temperature ranged from 23–26.5 °C. The solution was loaded into a 1 mL BD Luer-Lok syringe

 

(4.78 mm inner diameter). 200 proof ethanol was sprayed using a negative polarity for 5 min. The spray solution was then sprayed applying a positive polarity on the needle and the guard ring. The MNAs were placed onto a holding block where both the MNA and the holding block were grounded and insulated. The guard ring and all other conductive surfaces within the chamber were insulated with 2 mil Kapton polyimide tape. MNAs were sonicated in detergent and water for cleaning.

### 2.4. Experimental parameters

Efficient ESD was conducted and analyzed as previously reported in Park *et al.*[29] In brief, 200 proof ethanol was sprayed with a negative polarity (between 5–6 kV) applied to the needle tip for a minimum of 5 min prior to deposition on the substrate of interest. The negative pre-spray was applied whenever an instability arose in the spray or every 3 hours between sample collection. Sprays were then stabilized by applying a positive polarity voltage between 7.2–9.7 kV at a constant spray distance of 4 cm from the needle tip to the substrate. The guard ring was placed between the needle and the substrate, 2 cm from the needle tip, and held a constant voltage of 0.41 kV. All sprays flowed at 0.1 mL $h^{-1}$ for 60 min, corresponding to 50 μg total of GLS-5300 plasmid. Coating efficiency was measured by eluting the coated needles into 300 μL of deionized water and measuring the concentration of the coatings *via* Thermo Scientific NanoDrop 2000c. Low-magnification optical images were collected with a Dino-Lite AM73915MZT. High-magnification optical images were collected with a Leica DM2700 optical microscope using a 5× objective, with thicknesses on the needle bodies checked through a Filmetrics F40-EXR microreflectometer using polystyrene as a general model for the index of refraction.

### 2.5. Nanoindentation measurements

To measure the mechanical properties *via* nanoindentation load-controlled experiments were employed with a Berkovich tip on a NanoTest Vantage system. Samples were dropcast from spray solution to a thickness of several microns (as determined by microreflectometry) and dried in air. Then, single indent depth-controlled experiments were initially performed with pure plasmid to determine the maximum load at which <10% of the film thickness was achieved during this indentation cycle. The load corresponding to this ~10% depth (0.5 mN) was then prescribed as a maximum load during the actual experiments for all materials. A 5-300-5 load function used. This load function represents a five-second loading time, a five-minute hold time at the maximum load, and a five second unload time. Each sample was tested with 100 indents. The loading and unloading curves normalized to the values for DNA-only have been provided as ESI† Data Sets.

### 2.6. *In vitro* transfection of 293T cell

HEK293T cells were cultured in Dulbecco's modified Eagle's medium with 10 v/v% fetal bovine serum and 1 v/v% penicillin–streptomycin (Gibco, Grand Island, NY) at 37 °C with 5% $CO_2$. Cells were transfected in 96-well plate after reaching 80% confluency. Using FuGENE® 6 (Promega, Madison, WI) mediated transfection, cells were transfected with plasmid GFP using 3 : 1 reagent : plasmid GFP with a final volume of 100 μL per well. Wells with plasmid received 1.25 μg of GFP. After incubating for 24 h, wells were imaged using Olympus 1 × 80 microscope. Each condition was done in triplicate where 5 images were taken in random locations for each replicate.

### 2.7. Animals

Male Sprague Dawley rats (NTac-SD; murine pathogen free), aged 7–10 weeks, were purchased from Taconic Biosciences, Inc. (Germantown, NY) and were housed under 12–12 h light–dark cycle at room temperature. Animal housing and procedures were in accordance with guidelines established by the Rutgers University Institutional Animal Care and Use Committee under protocol IACUC-201800077. Rats were anesthetized using isoflurane. Upon anesthetization, rats were shaved with hair clippers (WAHL, Sterling, Il). Fur was further removed by applying a depilatory cream (Nair Hair Removal Lotion Softening Baby Oil, Ewing, NJ) for 5 min and then removed where the skin was then cleaned with 70% ethanol. Using a 28-gauge insulin syringe (Comfort Point, Exelin, Redondo Beach, CA), 50 μg of GLS-5300 was delivered in 50 μL of 1X PBS solution *via* Mantoux injection. 80 kPa of suction was then applied to the entire injection bleb or insertion site for 30 s using a trademarked device, GeneDerm (Model JM11, South Korea). The suction cup attachment had an inner diameter of 6 mm and rim thickness of 1 mm. Each rat ($n$ = 3) received a Mantoux-style injection, a vaccine-only coated MNA insertion, and a vaccine with excipients coated MNA insertion. All animals were sacrificed after 24 h of the experiment where the skin was excised at the site of the injection or insertion.

### 2.8. Immunohistochemistry

Excised skin was fixed in 10 w/v% formalin for 24 h at room temperature and then incubated in 10 w/v% sucrose in 1X PBS for cryopreservation. Tissue blocks were then embedded in optimal cutting temperature media and mounted onto electrostatically surface-treated glass slides. Each section was 10 μL in thickness. Slides were washed in 1X tris-buffered saline, 0.1 w/v% Tween 20 (TBST) before staining. Non-specific binding of sections was blocked using permeabilization and blocking buffer with normal goat serum. Sections were then incubated with MERS Coronavirus Spike Protein RBD Polyclonal Antibody primary antibody (Invitrogen, Waltham, MA) overnight at 4 °C and Goat anti-Rabbit IgG (H + L) Secondary Antibody, Alexa Fluor 546 (Invitrogen, Waltham, MA) for 30 min at room temperature. Primary and secondary antibody was diluted to 10 μg $mL^{-1}$ and 4 μg $mL^{-1}$, respectively, using antibody incubation buffer. Diamond anti-fade mounting media with DAPI (Invitrogen, Waltham, MA) was then used to stain and mount the slides before imaging. All slides were imaged using Olympus 1 × 80 microscope.

## 3. Results and discussion

### 3.1. Coating MNAs *via* ESD

Stainless-steel MNAs were grounded and placed on top of an insulated extractor ground to focus the charged droplets solely

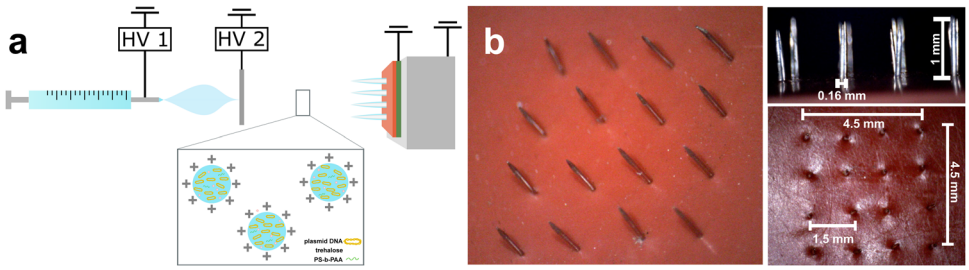


Fig. 1 (a) Schematic of ESD setup to coat MNAs with plasmid DNA. Positive polarity voltage is applied to the capillary and to the guard ring to focus the charged droplets towards the grounded MNA. Charged droplets include a plasmid DNA alone (DNA-only) or a mixture of plasmid DNA, trehalose, and PS-*b*-PAA (DNA + excipients). (b) MNAs were fabricated using 0.16 mm diameter acupuncture needles. Needles are 1 mm in length and spaced 1.5 mm apart. Each array has 16 needles total for a surface area of approximately 20 $mm^2$.

onto the needle surfaces, utilizing the optimized ESD setup as discussed in Park *et al.* (Fig. 1a).[20] These arrays were fabricated using acupuncture needles that were cut to 2 mm in length. A silicone sheet was placed on top of the needles such that only 1 mm remained exposed (Fig. 1b). Excipients were added to the DNA vaccine (DNA + excipients) to improve the stability of the DNA and the mechanical toughness on insertion. Pure plasmid DNA (DNA-only) was sprayed in addition to the excipient blend for the comparison of the two vaccine coatings. Measurements with NanoDrop ultraviolet-visible spectrophotometry indicated that no material was lost during the coating procedure for both DNA-only MNAs and DNA + excipients MNAs with apparent coating efficiencies measured to be 102 ± 0.13% and 104 ± 0.16%, respectively. Experimental parameters for all sprays can be found in Table S1 (ESI†) where the voltages are reported in a range as environmental conditions (*e.g.*, relative humidity) affect the voltage needed to achieve a stable Taylor cone-jet.[30]

### 3.2. *In vitro* transfection using electrosprayed GFP

Shear forces experienced during electrospray have been shown to damage fragile biomaterials and may damage DNA.[15,26] However, other studies report that high ethanol concentration, which collapses DNA, and low solution flow rates, which increases droplet size, may combat shear-induced fragmentation of the plasmids.[26,27] To assess whether plasmid DNA retains its functional ability, plasmid pEGFP-N1, encoding for the green fluorescent protein (GFP), was sprayed onto MNAs using both coating formulations: DNA-only (Fig. 2a) or DNA + excipients (Fig. 2b). Following ESD, the coatings were eluted into DI water and combined with FuGENE transfection reagent for *in vitro* transfection of HEK293T cells. Qualitatively, transfection with eluted pEGFP-N1 led to GFP expression that was comparable to transfection with stock plasmids, *i.e.* plasmid DNA that had not been coated onto microneedles (Fig. 2c). This result was observed for both DNA-only and DNA + excipients. We hypothesize that the combination of a high ethanol environment and a lowered flow rate is synergistic, contributing to decreased DNA damage during ESD leading to GFP expression. However, more studies are needed to confirm this interaction.

### 3.3. *In vivo* expression of electrosprayed GFP in rats

pEGFP-N1 sprayed onto MNAs was inserted into rat skin ($n$ = 1) for *in vivo* transfection (see Fig. 3 for experimental schematic). Both coating formulations were used for this experiment to assess the effect of the excipients. After insertion, the experimental site was subjected to a negative pressure of 80 kPa for

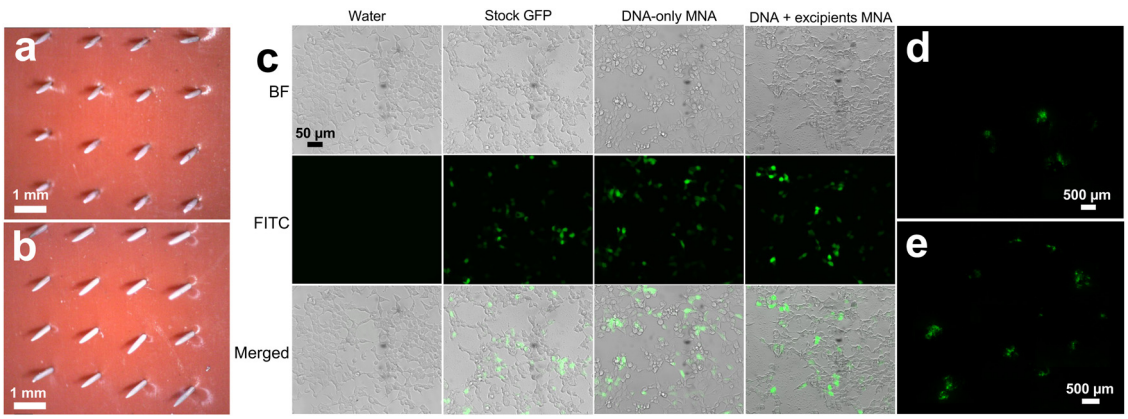


Fig. 2 Images of 4 × 4 MNA coated with (a) 50 μg of plasmid GFP (DNA-only MNA) and (b) 50 μg of plasmid GFP, 25 μg of trehalose, and 5 μg of PS-*b*-PAA (DNA + excipients MNA). (c) *In vitro* transfection of HEK293T cells using FuGENE 6. Images were taken 24 h after transfection. Coatings were eluted into DI water for transfection. Comparable expression levels are observed for cells transfected with sprayed GFP, with and without excipients, and the stock plasmid control. Fluorescent images of *in vivo* transfection of cells in rat skin using electrosprayed (d) plasmid GFP and (e) plasmid GFP, trehalose, and PS-*b*-PAA coated MNAs after 24 h. Green fluorescence spots correlate with the location of needle insertion sites in the tissue.

 

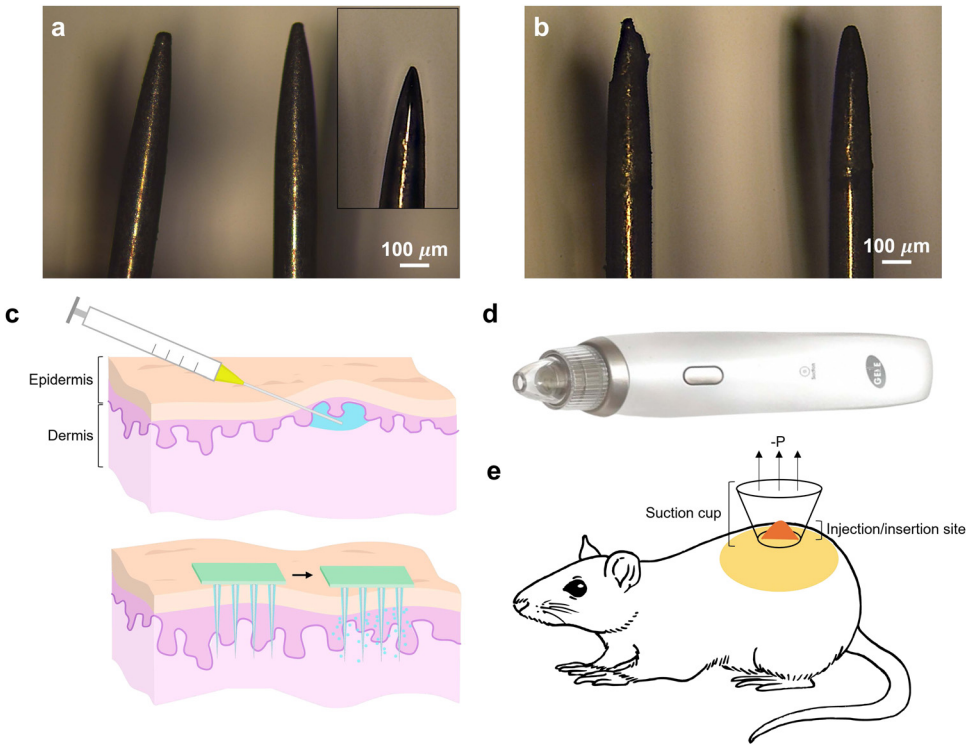


Fig. 3 High-magnification images of (a) 50 μg of plasmid vaccine and (b) 50 μg of plasmid vaccine, 25 μg of trehalose, and 5 μg of PS-*b*-PAA post water vapor smoothing. An uncoated MN is shown in the inset. (c) Methods implemented for intradermal delivery of vaccine using Mantoux injection (top) and coated microneedle array (bottom), targeting the region between the viable epidermis and dermis. Blue around microneedles indicate the sprayed coating and dispersion after insertion. (d) Suction device for vaccine site treatment. (e) Schematic for experimental setup where negative pressure (−*P*) is applied to the entire injection/insertion site.

30 s using the device in Fig. 3b to enhance transfection as described in our previous work (Fig. 3c).[31,32] Coating formulation is integral for creating an excipient matrix that can help preserve the payload material while also avoiding coating delamination at the surface of the skin. By blending these excipients with a plasmid DNA vaccine, we aimed to avoid delamination at the surface while conserving the functionality of DNA. Fig. 2d and e show expression of sprayed DNA-only MNA and sprayed DNA + excipients MNA in rat skin, respectively, thus demonstrating the viability of electrosprayed pEGFP-N1 for transgene expression. When comparing the expression of the two coating formulations in Fig. 2d and e, it appears that more insertion sites are expressing GFP for DNA + excipients, suggesting more effective insertion and release (Fig. S1, ESI†). Trehalose is a sugar commonly used as a stabilizer for more fragile biological materials during the electrospray process[15,33] and can also preserve the structure of DNA and proteins against extreme temperatures.[34,35] However, brittle coatings, such as sugar complexes, can delaminate from the surface of the needle during insertion.[3,36] To help counteract this, PS-*b*-PAA was used as PS-*b*-PAA is a biocompatible polymer frequently used for drug delivery applications to improve the toughness of biomaterials to minimize deformation of the material.[37,38] This can be seen in nanoindentation of dropcast films of vaccine DNA-only, DNA blended with trehalose only, and DNA + excipients (Fig. S2, ESI†). While all three formulations possessed similar response during loading, the response of the DNA blended with trehalose alone was characteristically less viscoelastic, having the least creep in load-displacement curves seen in Fig. S2 (ESI†), while the DNA + Excipients was the most viscoelastic of the samples tested. Viscoelasticity in polymers correlates with fracture resistance[39] *via* energy absorption, stress relaxation *etc.*, especially considering how similar the other features of the loading and unloading curves are. The area under the curve represents the material's capacity to absorb energy prior to fracturing, with a larger area indicating greater fracture resistance and enhanced toughness. In Fig. S2 (ESI†), the area under the curve for DNA + excipients is larger than that of DNA and DNA blended with trehalose. Compared to DNA-only, DNA + excipients has a 3.59% increase in area, and in conjunction with a longer relaxation time, the material exhibits favorable viscoelastic properties, enhancing energy absorption and fracture resistance. We suspect the combined interactions of trehalose and PS-*b*-PAA increases the stability of the plasmid as well as the coating properties, thus improving GFP expression from the coated needles.

### 3.4. Immunohistochemistry results of MERS-CoV vaccination

*In vivo* transfection ($n$ = 3 rats) was performed with MNAs coated with 50 μg of MERS-CoV vaccine with both coating formulations. The sprayed coatings were smoothed using water vapor and acetone prior to any *in vivo* experimentation (Fig. 3a and b), as smoothing the coating can additionally mitigate

delamination. Greater accumulation can be seen near the tips of the needles, as confirmed by microreflectometry (Fig. S3 and S4, ESI†), with the DNA + Excipients showing a thicker film consistent with the higher total of solids mass deposited to maintain the same DNA dose. Two intradermal methods were employed to deliver the vaccine into the rat (Fig. 3b): intradermal Mantoux injection and coated MNA insertion. Suction was applied to injection and insertion sites after needle removal (Fig. 3d and e). The animals were sacrificed after 24 h. The experimental sites were excised and prepared for cryosectioning and immunostaining.

The sections were stained with an anti-MERS-CoV primary antibody targeting the receptor binding domain (RBD) within the spike protein. Fluorescent green latex beads (30 μm diameter) were sprayed with the vaccine and excipients to assist with locating the MNA insertion sites as well as estimating the depth that the needles penetrate (Fig. 4a and b, and Fig. S5, ESI†). Although the depth of needle penetration was approximately 300 μm for both DNA-only MNA and DNA + excipients MNA, differences in the dispersion of the beads were observed. For needles coated with DNA-only, beads appeared to remain close to the needle and at high density through fluorescent imaging (Fig. 4a), whereas with excipients, beads were dispersed further away from the needles and demonstrated a more diffuse fluorescence profile (Fig. 4b). Although PS-*b*-PAA can mechanically toughen the coating,[38] the carboxyl groups in PAA can also behave as grafts or branches, creating hairy micelles. Surfactants are commonly used in MNA coating formulations to lower surface tension and have also been shown to improve the dissolution of the coating upon administration, thus aiding in the dissolution of the coating from the needles.[40] In the case of DNA + excipients MNA, we suspect the PS-*b*-PAA may be contributing to the more diffuse beads, and thus greater diffusion of the coating, seen in Fig. 4b. However, more experimentation is necessary to fully understand the effect of the excipients on dissolution and diffusion kinetics beyond the qualitative analysis of these images.

Sections were immunolabeled with anti-MERS-CoV spike protein RBD along with DAPI to label cell nuclei and to assist in differentiating the layers of the epidermis and dermis. Fluorescence was generally observed in all cases in the stratum corneum (SC), including control conditions without vaccine, and this was deemed to be non-specific staining due to autofluorescence (Fig. 4c). In all conditions where the vaccine was introduced, labeling was observed deeper in the epidermis. Following Mantoux-style injection, or "ID injection", immunolabeled RBD protein was primarily located in the upper levels of the epidermis, inferior to the SC. Expression levels varied and were often observed as high-intensity labeling within cells. In contrast, following vaccination with coated MNAs with and without excipients, the immunolabeling was primarily in the deeper epidermis near the basal lamina. In these cases, expression was more uniform and diffuse across cells in the lower epidermis. No substantial differences were observed in immunolabeling patterns between electrosprayed vaccine with and without excipients. Whether the electrosprayed DNA vaccine on MNAs elicits an equivalent immune response as intradermal injections after application of suction remains to be investigated in a future study with antibody titers.

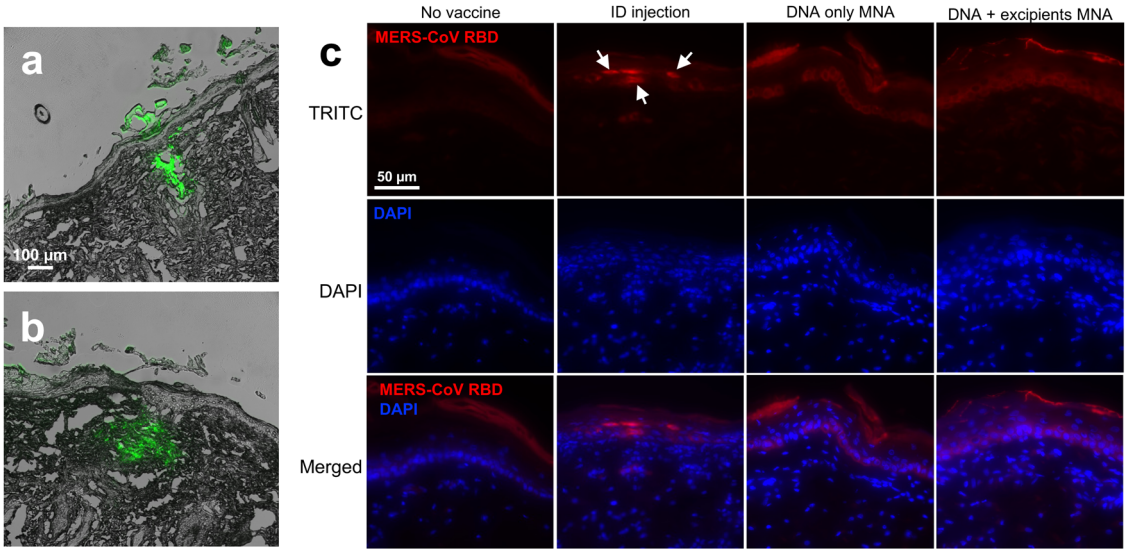


Fig. 4 Fluorescent images of tissue cross sections. MNAs were sprayed with fluorescent latex beads and (a) vaccine-only and (b) vaccine + excipients and then inserted into tissue. Green fluorescence indicates the location of latex beads where dispersion of the beads with excipients diffused further from the needle compared to the beads with the vaccine alone. (c) Immunofluorescence staining of MERS-CoV Spike protein RBD in rat skin tissue where red fluorescence denotes MERS-CoV RBD protein and blue fluorescence denotes DAPI staining of skin cell nuclei. "No vaccine" tissue did not receive vaccine nor suction treatment. "ID injection" represents intradermal injection of MERS-CoV vaccine with suction post-treatment, "DNA-only MNA" represents MNA injection coated with MERS-CoV vaccine with suction post-treatment, and "DNA + excipients MNA" represents MNA injection coated with MERS-CoV vaccine, trehalose, and PS-*b*-PAA with suction post-treatment. Expression levels were variable in ID injection as immunolabeling intensity was higher within cells, indicated by arrows, while coated MNAs resulted in more uniform expression throughout the lower epidermis.

 

## 4. Conclusion

MNAs are an emerging technology for delivering therapeutics intradermally. ESD is a coating technique capable of precise thin film coating on these arrays, which can prove to be advantageous for costly or sparsely available therapeutics. In general, MNAs are less costly to produce as there are few components involved in its mass manufacturing while ESD is a low-cost, rapid process where the combination of the two could lead to promising economic advantages.[1,41] In this work, we demonstrated that ESD is a viable method to coat biologically active plasmid DNA onto MNAs despite concerns of causing damage to fragile materials where the viability of sprayed DNA was shown in both HEK293T cell transfection and rat tissue sections *via* immunohistochemistry. The relevance of this application extends to an alternative way to distribute therapeutics without requiring cold chain supply, all while reducing material waste which could be essential during vaccine rollout for pandemics. Although the immune response was not quantified in this study, *in vivo* results, suggest that DNA vaccine-coated MNAs *via* ESD are capable of protein expression in response to the vaccine. Moreover, the combination of DNA vaccines with MNAs could be a viable and competitive method for vaccine and therapeutics delivery compared to traditional hypodermic needle injections where coating MNAs through ESD may offer a more rapid and efficient coating process.

## Author contributions

SHP, JPS, and DIS conceptualized the experimental design. SHP, IRS, NJC, YM, ST, and EOL performed the experiments. SHP and JPS prepared the original draft. SHP prepared visuals. All other authors contributed to reviewing and editing the original and/or revised draft.

## Data availability

The data supporting this article have been included as part of the ESI.†

## Conflicts of interest

JPS and SHP are inventors on patents and patent applications on electrospray technology licensed to GeneOne Life Science. JPS is cofounder of Plumajet Inc., which seeks to commercialize electrospray technologies from his lab. All other authors decare no competing interests.

## Acknowledgements

This research was partially funded by GeneOne Life Science, who also provided plasmid materials. SHP and JPS acknowledge funding from the Rutgers Mary W. Raisler Distinguished Teaching Chair.

## References

1 J. Arya and M. R. Prausnitz, Microneedle patches for vaccination in developing countries, *J. Controlled Release*, 2016, **240**, 135–141.
2 E. Larrañeta, R. E. M. Lutton, A. D. Woolfson and R. F. Donnelly, Microneedle arrays as transdermal and intradermal drug delivery systems: Materials science, manufacture and commercial development, *Mater. Sci. Eng., R*, 2016, **104**, 1–32.
3 H. S. Gill and M. R. Prausnitz, Coating formulations for microneedles, *Pharm. Res.*, 2007, **24**(7), 1369–1380.
4 A. Vrdoljak, M. G. McGrath, J. B. Carey, S. J. Draper, A. V. S. Hill and C. O'Mahony, *et al.*, Coated microneedle arrays for transcutaneous delivery of live virus vaccines, *J. Controlled Release*, 2012, **159**(1), 34–42.
5 R. T. Kenney, S. A. Frech, L. R. Muenz, C. P. Villar and G. M. Glenn, Dose Sparing with Intradermal Injection of Influenza Vaccine, *N. Engl. J. Med.*, 2004, **351**(22), 2295–2301.
6 P. E. Laurent, H. Bourhy, M. Fantino, P. Alchas and J. A. Mikszta, Safety and efficacy of novel dermal and epidermal microneedle delivery systems for rabies vaccination in healthy adults, *Vaccine*, 2010, **28**(36), 5850–5856.
7 M. Kurakula and G. Rao, Pharmaceutical assessment of polyvinylpyrrolidone (PVP): As excipient from conventional to controlled delivery systems with a spotlight on COVID-19 inhibition, *J. Drug Delivery Sci. Technol.*, 2020, **60**, 102046.
8 S. M. Bal, J. Caussin, S. Pavel and J. A. Bouwstra, In vivo assessment of safety of microneedle arrays in human skin, *Eur. J. Pharm. Sci.*, 2008, **35**(3), 193–202.
9 U. Angkawinitwong, A. J. Courtenay, A. M. Rodgers, E. Larraneta, H. O. McCarthy and S. Brocchini, *et al.*, A Novel Transdermal Protein Delivery Strategy via Electrohydrodynamic Coating of PLGA Microparticles onto Microneedles, *ACS Appl. Mater. Interfaces*, 2020, **12**(11), 12478–12488.
10 Y. C. Kim, J. H. Park and M. R. Prausnitz, Microneedles for drug and vaccine delivery, *Adv. Drug Delivery Rev.*, 2012, **64**(14), 1547–1568.
11 F. Fan, X. Zhang, Z. Zhang, Y. Ding, L. Wang and X. Xu, *et al.*, Potent immunogenicity and broad-spectrum protection potential of microneedle array patch-based COVID-19 DNA vaccine candidates encoding dimeric RBD chimera of SARS-CoV and SARS-CoV-2 variants, *Emerging Microbes Infect.*, 2023, **12**(1), 2202269.
12 S. Zhang, S. Zhao, X. Jin, B. Wang and G. Zhao, Microneedles Improve the Immunogenicity of DNA Vaccines, *Hum. Gene Ther.*, 2018, **29**(9), 1004–1010.
13 S. E. Law, Agricultural electrostatic spray application: a review of significant research and development during the 20th century, *J. Electrost.*, 2001, **51–52**, 25–42.
14 J. A. Tapia-Hernandez, P. I. Torres-Chavez, B. Ramirez-Wong, A. Rascon-Chu, M. Plascencia-Jatomea and C. G. Barreras-Urbina, *et al.*, Micro- and nanoparticles by electrospray: advances and applications in foods, *J. Agric. Food Chem.*, 2015, **63**(19), 4699–4707.
15 V. N. Morozov, Electrospray deposition of biomolecules, *Adv. Biochem. Eng./Biotechnol.*, 2010, **119**, 115–162.

16 R. A. Green-Warren, A. L. Fassler, A. Juhl, N. M. McAllister, A. Huth and M. Arkhipov, *et al.*, Self-limiting electrospray deposition (SLED) of porous polyimide coatings as effective lithium-ion battery separator membranes, *RSC Appl. Polym.*, 2024, **2**, 1074–1081.

17 Y.-X. Yin, S. Xin, L.-J. Wan, C.-J. Li and Y.-G. Guo, Electrospray Synthesis of Silicon/Carbon Nanoporous Microspheres as Improved Anode Materials for Lithium-Ion Batteries, *J. Phys. Chem. C*, 2011, **115**(29), 14148–14154.

18 T. Fukuda, A. Toda, K. Takahira, D. Kuzuhara and N. Yoshimoto, Improved performance of organic photovoltaic cells with PTB7-Th:PC71 BM by optimized solvent evaporation time in electrospray deposition, *Org. Electron.*, 2017, **48**, 96–105.

19 Q. Zeng, L. Hu, J. Cui, T. Feng, X. Du and G. Jin, *et al.*, High-Efficiency Aqueous-Processed Polymer/CdTe Nanocrystals Planar Heterojunction Solar Cells with Optimized Band Alignment and Reduced Interfacial Charge Recombination, *ACS Appl. Mater. Interfaces*, 2017, **9**(37), 31345–31351.

20 S. H. Park, L. Lei, D. D'Souza, R. Zipkin, E. T. DiMartini and M. Atzampou, *et al.*, Efficient electrospray deposition of surfaces smaller than the spray plume, *Nat. Commun.*, 2023, **14**(1), 4896.

21 K. Jittavanich, C. B. Clemons, K. L. Kreider, M. Aljarrah, E. Evans and G. W. Young, Modeling, simulation and fabrication of coated structures using the dip coating technique, *Chem. Eng. Sci.*, 2010, **65**(23), 6169–6180.

22 Z. Zhang, F. Peng and K. G. Kornev, The Thickness and Structure of Dip-Coated Polymer Films in the Liquid and Solid States, *Micromachines*, 2022, **13**(7), 982.

23 Y. C. Kim, F. S. Quan, R. W. Compans, S. M. Kang and M. R. Prausnitz, Stability kinetics of influenza vaccine coated onto microneedles during drying and storage, *Pharm. Res.*, 2011, **28**(1), 135–144.

24 A. Jaworek, Electrospray droplet sources for thin film deposition, *J. Mater. Sci.*, 2006, **42**(1), 266–297.

25 D. A. Kovacevich, L. Lei, D. Han, C. Kutznetsova, H. Lee and J. P. Singer, Self-Limiting Electrospray Deposition for the Surface Modification of Additively Manufactured Parts, *ACS Appl. Mater. Interfaces*, 2020, **12**(18), 20901–20911.

26 Y. M. Shlyapnikov, E. A. Shlyapnikov and V. N. Morozov, Reversible and Irreversible Mechanical Damaging of Large Double-Stranded DNA upon Electrospraying, *Anal. Chem.*, 2016, **88**, 7295–7301.

27 S. Marchetti, G. Onori and C. Cametti, Ethanol-induced compaction of DNA: a viscosimetry and dynamic light scattering study, *Philos. Mag.*, 2007, **87**, 525–534.

28 K. Modjarrad, C. C. Roberts, K. T. Mills, A. R. Castellano, K. Paolino and K. Muthumani, *et al.*, Safety and immunogenicity of an anti-Middle East respiratory syndrome coronavirus DNA vaccine: a phase 1, open-label, single-arm, dose-escalation trial, *Lancet Infect. Dis.*, 2019, **19**(9), 1013–1022.

29 S. H. Park, L. Lei, D. D'Souza, R. Zipkin, E. T. DiMartini and M. Atzampou, *et al.*, Efficient Electrospray Deposition of Surfaces Smaller than the Spray Plume, *Nat. Commun.*, 2023, **14**, 4896.

30 L. Lei, D. A. Kovacevich, M. P. Nitzsche, J. Ryu, K. Al-Marzoki and G. Rodriguez, *et al.*, Obtaining Thickness-Limited Electrospray Deposition for 3D Coating, *ACS Appl. Mater. Interfaces*, 2018, **10**(13), 11175–11188.

31 E. O. Lallow, N. C. Jhumur, I. Ahmed, S. B. Kudchodkar, C. C. Roberts and M. Jeong, *et al.*, Novel suction-based in vivo cutaneous DNA transfection platform, *Sci. Adv.*, 2021, **7**(45), eabj0611.

32 N. C. Jhumur, E. O. Lallow, C. J. Nachtigal, D. Yeo, I. Kwon and Y. K. Park, *et al.*, Tissue Tension and Strain as Indicators of Suction-mediated Cutaneous DNA Transfection: A Parametric Study, *Adv. Ther.*, 2024, **7**(6), 2400055.

33 V. N. Morozov and T. Y. Morozov, Electrospray Deposition as a Method To Fabricate Functionally Active Protein Films, *Anal. Chem.*, 1999, **71**, 1415–1420.

34 M. Zhang, H. Oldenhof, B. Sydykov, J. Bigalk, H. Sieme and W. F. Wolkers, Freeze-drying of mammalian cells using trehalose: preservation of DNA integrity, *Sci. Rep.*, 2017, **7**(1), 6198.

35 D. Barreca, G. Lagana, S. Magazu, F. Migliardo, G. Gattuso and E. Bellocco, FTIR, ESI-MS, VT-NMR and SANS study of trehalose thermal stabilization of lysozyme, *Int. J. Biol. Macromol.*, 2014, **63**, 225–232.

36 H. S. Gill and M. R. Prausnitz, Coated microneedles for transdermal delivery, *J. Controlled Release*, 2007, **117**(2), 227–237.

37 C. Wang, Y. Mao, D. Wang, Q. Qu, G. Yang and X. Hu, Fabrication of highly ordered microporous thin films by PS-*b*-PAA self-assembly and investigation of their tunable surface properties, *J. Mater. Chem.*, 2008, **18**(6), 683–690.

38 S. Y. Yang, E. D. O'Cearbhaill, G. C. Sisk, K. M. Park, W. K. Cho and M. Villiger, *et al.*, A bio-inspired swellable microneedle adhesive for mechanical interlocking with tissue, *Nat. Commun.*, 2013, **4**(1), 1702.

39 W. G. Knauss, A review of fracture in viscoelastic materials, *Int. J. Fract.*, 2015, **196**(1), 99–146.

40 Q. K. Anjani, A. H. B. Sabri, E. Utomo, J. Domínguez-Robles and R. F. Donnelly, Elucidating the Impact of Surfactants on the Performance of Dissolving Microneedle Array Patches, *Mol. Pharmaceutics*, 2022, **19**(4), 1191–1208.

41 A. Jaworek and A. T. Sobczyk, Electrospraying route to nanotechnology: An overview, *J. Electrost.*, 2007, **66**, 197–219.

 